Earth and Planetary Science Letters 279 (2009) 255–262

Contents lists available at ScienceDirect

Earth and Planetary Science Letters

journal homepage: www.elsevier.com/locate/epsl

3D shear velocity structure beneath the Gulf of California from Rayleigh wave dispersion

X. Zhang [a,*], H. Paulssen [a], S. Lebedev [a,b], T. Meier [c]

[a] Utrecht University, Department of Earth Science, P.O. Box 800021, 3508 TA, Utrecht, The Netherlands
[b] Dublin Institute for Advanced Studies, Geophysics Section, 5 Merrion Square, Dublin 2, Ireland
[c] Ruhr-University Bochum, Department of Geosciences, Universitaetsstr. 150, NA3/165, Bochum, D-44780, Germany

ARTICLE INFO

Article history:
Received 30 June 2008
Received in revised form 19 November 2008
Accepted 2 January 2009
Available online 1 February 2009

Editor: C.P. Jaupart

Keywords:
Gulf of California
Rayleigh waves
shear velocity
tomography
tectonics

ABSTRACT

Active extension in the Gulf of California is characterized by the transition from continental rifting to seafloor spreading. Puzzling variations in the patterns of both tectonics and magmatism are observed along the length of the gulf and are likely to be related to mantle heterogeneity. Regional-scale mantle structure, however, has been difficult to constrain due to the lack of broadband seismic stations in the region. In this study we utilized new data from the deployment of the NARS-Baja array and other networks, and computed a three-dimensional shear-speed model of the upper mantle beneath the region. Applying a combination of cross-correlation analysis and multimode waveform inversion, we measured interstation Rayleigh wave dispersion for 450 pairs of stations in a broad period range of 9–250 s. We computed phase velocity maps and then inverted the phase-velocity data for shear-speed structure. Our results suggest that the location of the transition from seafloor spreading (South) to continental rifting (North) in the Gulf of California, as well as differences in volcanism across Baja California and the gulf, can be explained by heterogeneity in the upper mantle, in particular by the presence of a slab remnant beneath the south-central part and an absence of such a slab remnant beneath the northern part of the gulf.

1. Introduction

The Gulf of California, which forms a part of the Pacific-North American plate boundary, is currently extending by means of active rifting. It links the East Pacific Rise and the San Andreas transform fault system, and accommodates a transition from oceanic spreading to continental extension. Because the two types of rifting are juxtaposed, it is one of the few regions where we can investigate the evolution of a rift. It is unclear what causes the differences in the style of rifting between the southern part of the gulf, characterized by oceanic spreading centers and transform faulting (Lonsdale, 1989; Lizarralde et al., 2007), and its northern part, where diffuse continental deformation is occurring (Nagy and Stock 2000; Oskin and Stock, 2003; González-Fernández et al., 2005). These variations cannot be explained by variations in the amount of deformation: the South and North have experienced roughly the same amount (~300 km) of oblique Northwest–Southeast extension since the opening of the gulf at about 6 Ma (Persaud et al., 2003). Moreover, seismic refraction experiments have revealed that basins in the southern and central gulf vary from wide to narrow rifts over small distances (~200 km) (Lizarralde et al., 2007).

The formation of the Gulf of California is associated with the cessation of subduction of the Farallon plate beneath the North American continent, which occurred approximately 12 Myr ago at the latitudes of central Baja California (Mammerickx and Klitgord, 1982; Lonsdale, 1991; Michaud et al., 2006). When the subduction of the (Farallon-derived) Guadalupe and Magdalena microplates beneath Baja California ceased, the spreading at the mid-ocean ridge segments separating these microplates from the Pacific Plate also ended (Lonsdale, 1991; Stock and Lee, 1994). The Farallon–North American convergence then gave way to Pacific–North American transform motion, accommodated along the San Benito and Tosco–Abreojos faults close to the former trench (Fig. 1). The extensional component of the new Pacific–North American plate motion was taken up in the back-arc region, east of the Baja Peninsular Range and west of the Sierra Madre Occidental batholiths. This region, known as the Gulf Extensional Province, underwent East–Northeast extension from 12 Ma to 6 Ma forming a so-called 'proto-gulf' (Karig and Jensky, 1972; Stock, and Hodges, 1989; Henry and Aranda-Gomez, 2000). At approximately 6 Ma, much of the Pacific–North American transform motion along the San Benito and Tosco–Abreojos faults ended, moved inland, and was taken up in the gulf area along transform faults and pull-apart basins (Lonsdale, 1991; Oskin and Stock, 2003). Approximately 90% of the present Pacific–North American plate motion (of 51 mm/yr) is taken up by the northwest extension in the gulf (Plattner et al., 2007).

* Corresponding author. Tel.: +31 30 2535192; fax: +31 30 2532648.
E-mail address: zxm@geo.uu.nl (X. Zhang).

0012-821X/$ – see front matter © 2009 Elsevier B.V. All rights reserved.
doi:10.1016/j.epsl.2009.01.003

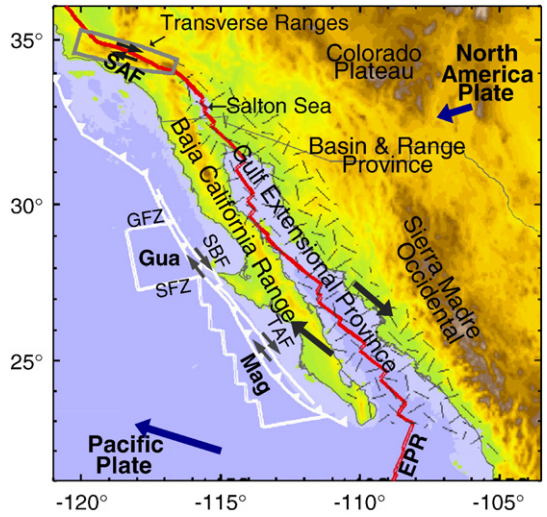

Fig. 1. Tectonic map of the Gulf of California region. The main tectonic provinces are Baja California Range, Gulf Extensional Province (hatched), Transverse Ranges (marked by gray box), Basin and Range Province, Sierra Madre Occidental and Colorado Plateau. Present-day plate boundary is shown as a red line. Inactive plate boundaries are shown as white lines. SAF—San Andreas Fault; EPR—East Pacific Rise; SBF—San Benito Fault; TAF—Tosco Abreojos Fault; GFZ—Guadalupe Fracture Zone; SFZ—Shirley Fracture Zone; Gua—Guadalupe microplate; Mag—Magdalena microplate. Thick arrows indicate plate motions (absolute plate motion in blue, relative plate motion in black) predicted by global plate motion model HS3-NUVEL1A (Gripp and Gordon, 2002).

The magmatism in Baja California and the Gulf of California is closely linked to the tectonic history of the region. The Baja Peninsular Range, a subduction-related calc-alkaline volcanic arc, was formed approximately between 24 and 11 Ma, along a large part of what is currently the Baja California peninsula (Gastil et al., 1979; Hausback, 1984; Sawlan and Smith, 1984). This volcanism was progressively extinguished due to the southward migration of the Pacific–Farallon–North American triple junction, the migration changing the convergent plate boundary into a transform one (e.g., Sawlan, 1991). A slab window, an area without slab beneath the continent, was formed beneath the northern part of Baja California (Dickinson and Snyder, 1979; Severinghaus and Atwater, 1990; Atwater and Stock, 1998). At 12 Ma, when the Guadalupe and Magdalena microplates stopped subducting, a change occurred in the magmatism. The calc–alkaline form in central and southern Baja California gave way to other types of magmatism in various volcanic fields. The magmas produced include adakites derived from partial melting of subducted oceanic crust, magnesian andesites from a mantle metasomatized by slab-derived melts, and tholeiitic basalts without a (clear) subduction signature (e.g. Aguillón-Robles et al., 2001; Benoit et al., 2002; Calmus et al., 2003; Conly et al., 2005; Pallares et al., 2007). Tholeiitic lavas have been erupting in the Gulf of California since the initiation of rifting at ca. 12 Ma. Their geochemical signature ranges from tholeiites, typical of an intraplate setting (similar to ocean island basalts and continental flood basalts), to those typical of mature oceanic rifting (mid-ocean ridge basalts) depending on their location and on the stage of rifting at the time of eruption (Sawlan, 1991).

Understanding the evolution of the Gulf of California requires knowledge of processes in the mantle. Mantle temperature and composition control crustal extension through their effects both on flow in the mantle and crust and on magmatism. Seismic studies to date revealed anomalously low mantle shear velocities down to 250 km depth in the entire Gulf of California area (e.g. Lebedev and van der Hilst, 2008; Nettles and Dziewonski, 2008; van der Lee and Frederiksen, 2005). Lack of seismic stations in the area, however, has precluded resolution at the scale comparable to that of the observed variations in the style of rifting and magmatism.

In 2002, the NARS–Baja network of 19 broadband seismic stations was deployed along the perimeter of the Gulf of California (Trampert et al., 2003). Zhang et al. (2007) used the data from this network to measure Rayleigh wave phase velocities and computed azimuthally anisotropic phase-velocity maps for a broad period range. In this study we expand the study area so as to image the structure of the gulf in a larger regional context and invert the phase-velocity maps for three-dimensional shear-velocity structure. Recent results on the crustal structure (Persaud et al., 2007; Lizarralde et al., 2007) provide essential information and are incorporated into the inversion. Our most important result is the finding of a relatively high shear-velocity anomaly in the mantle beneath the central part of the Gulf of California, which we interpret to be a remnant of the subducted Guadalupe slab.

2. Method and data

We constrain the shear-velocity structure beneath the Gulf of California with surface–wave dispersion measurements. The

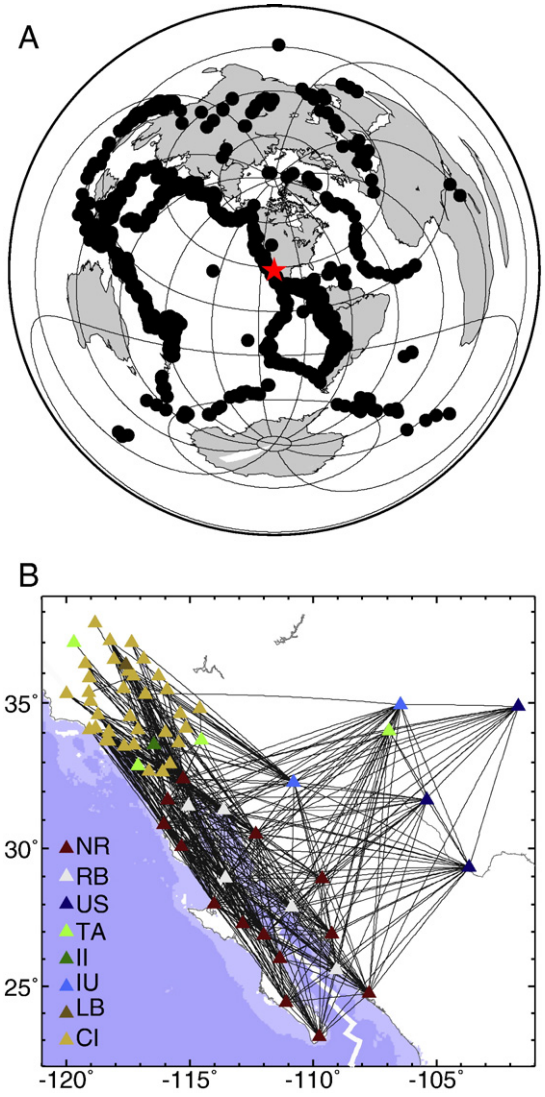

Fig. 2. Events and path distribution. Top: Event distribution. Bottom: Stations and ray path coverage. NR — NARS, the Network of Autonomously Recording Seismographs, Utrecht University, The Netherlands; RB — RESBAN, the Red Sísmica de Banda Ancha network, CICESE, Mexico; US — National Seismic Network, ANSS Backbone of the USGS/NEIC and USGS/ASL and Earthscope Project of IRIS, USA; TA — USArray Transportable Array, from Earthscope Project, USA; II — IRIS/IDA Network, University of California, Scripps Institute of Oceanography, USA; IU — IRIS/USGS Network, USGS Albuquerque Seismological Laboratory, USA; LB — Leo Brady Network, Sandia National Laboratory, USA; CI — The Caltech Regional Seismic Network, California Institute of Technology, USA.

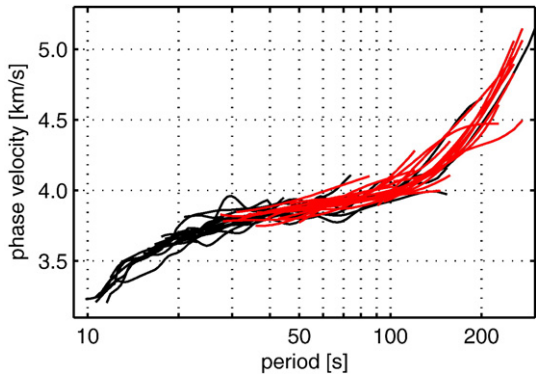

Fig. 3. Phase velocity measurements for the path between station NE70 and station TOV. Red curves are phase velocity measurements obtained by AMI; black curves are phase velocity measurements obtained by the two-station method.

interstation fundamental mode Rayleigh wave phase velocities were measured using the data recorded at stations of the NARS–Baja network and other stations in the vicinity of the gulf (see Fig. 2). The phase velocity curves were obtained by two approaches: a cross-correlation implementation of the two-station method as described by Meier et al. (2004) and the automated multimode inversion (AMI) (Lebedev et al., 2005). The two-station method relies on the cross-correlation of vertical component seismograms for events that are located within 7 degrees of the great circle between the two stations. The method involves frequency-dependent filtering and weighting; the phase velocity curve is interactively selected in the frequency domain. The advantage of the method is that it enables measurements at relatively high frequencies (periods down to 10 s and shorter). AMI is a waveform inversion technique that uses mode summation to generate synthetic seismograms and fits the parts of seismograms that are free from noise and scattered waves. Because it is a multi-mode waveform fitting technique, it can separate the relatively long-period fundamental mode from higher mode contamination. The interstation phase velocities are obtained from the dispersion curves of events recorded by stations that share the same great circle path (within 7°). This method is fully automated and fast, but it usually does not yield the higher frequency parts of the curves due to scattering and stringent selection criteria. We found that the phase velocity curves obtained with the two methods are generally consistent; cross-correlation measurements often extend to higher frequencies, whereas AMI measurements yield lower frequency results. We used cross-correlation measurements for paths across and around the gulf because their higher frequency content provides more constraints on the shallow structure, i.e. the crustal and uppermost mantle structure. AMI was used more extensively for the outer regions with paths to U.S. stations, so that the structure of the gulf could be interpreted in a broader regional setting. The final dispersion curves for each station pair were obtained as averages over many phase velocity curves measured using signal from different events, usually in a number of source regions, recorded at both stations.

The interstation approach is based on the assumption that surface waves propagate along the great-circle path so that the phase velocity curve is representative of the structure between the two stations. However, finite-frequency effects, such as off great-circle propagation, multipathing, and scattering (Prindle and Tanimoto, 2006; Pedersen, 2006), can cause biased estimates of the phase velocities, especially at short periods. This effect is reduced by averaging over phase velocity curves measured using signal from a large number of events. In addition, we checked that the measurements using surface waves arriving from the two opposite propagation directions were in agreement and then discarded biased measurements. For some station pairs systematic differences were observed between the measurements for the two opposite propagation directions at periods shorter than 30 s. We discarded the biased measurements, which are recognized by their higher apparent phase velocities, to obtain more reliable estimates of the dispersion curves (Pedersen, 2006; Zhang et al., 2007).

We analyzed Rayleigh wave data of earthquakes between April 2002 and the end of 2005 with moment magnitudes larger than 5. In total, 11,566 vertical component seismograms from 1192 events, recorded at 64 broadband stations, were used for the measurement of 450 interstation phase velocity curves. Fig. 2 shows the distribution of the events as well as the locations of the stations, together with the path distribution. A representative example, which shows the

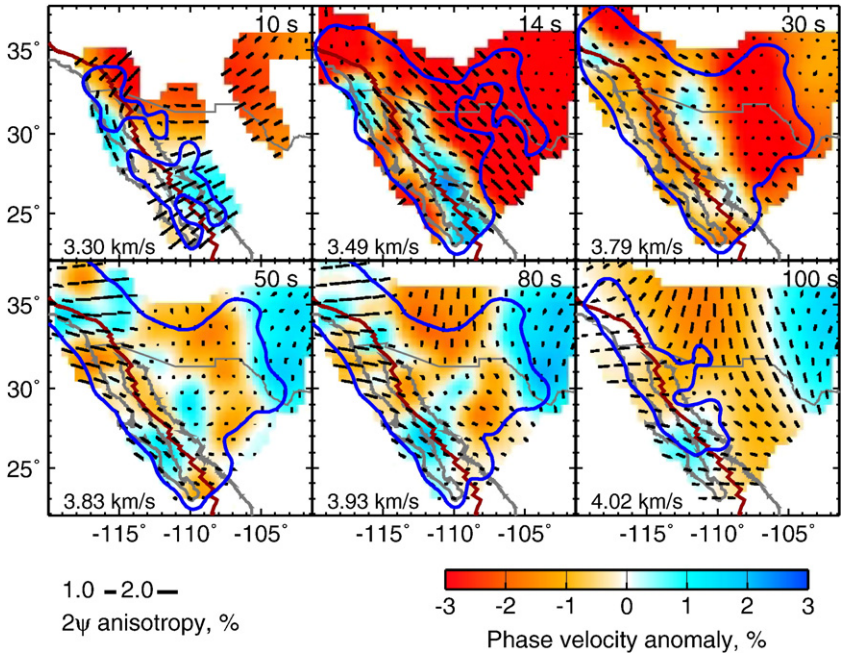

Fig. 4. Rayleigh wave phase velocities anomaly maps. The period is shown in the upper right corner and the reference phase velocity is in the lower left corner of each phase map. The colors indicate the isotropic anomalies and the black bars indicate the fast-propagation directions and the strength of the 2Ψ azimuthal anisotropy. The red line marks the location of the plate boundary. The blue contours delineate the regions of high resolution (see text) in each map.

agreement between the phase velocity measurements obtained by the two approaches, is shown in Fig. 3. It also illustrates the difference in frequency ranges of the measurements provided by the two different methods. The final phase velocity curves were obtained as the average of at least 8 individual curves with a minimum of 5 measurements per period. For most paths we had more than 20 phase velocity measurements averaged into robust dispersion curves. The measurements provide sufficient azimuthal coverage to allow the construction of phase velocity maps that include azimuthal anisotropy. Smith and Dahlen (1973) showed that the phase velocity in a layered weakly anisotropic medium depends on the propagation direction as

$$\frac{dc}{c}(T,\Psi) = \alpha_0(T) + \alpha_1(T)\cos 2\Psi + \alpha_2(T)\sin 2\Psi + \alpha_3(T)\cos 4\Psi + \alpha_4(T)\sin 4\Psi, \quad (1)$$

where dc/c is the relative phase velocity perturbation, T the period and Ψ the azimuth of wave propagation. The coefficient α_0 is the isotropic phase velocity perturbation; α_1, α_2, α_3 and α_4 parameterize azimuthal anisotropy. Adopting an approach similar to that of Lebedev and van der Hilst (2008), we inverted our dispersion curves for the isotropic phase velocity perturbations and the four anisotropy coefficients at the knots of a triangular grid with a nearly-uniform spacing of around 100 km and used LSQR (Paige and Saunders, 1982) with smoothing and slight norm damping to compute phase velocity maps at 32 periods, ranging from 9 to 250 s. We found that the isotropic component of the model can be resolved with a higher resolution compared to the anisotropic component, as is usual in anisotropic tomographic inversions (e.g. Lebedev and van der Hilst, 2008). At the shortest (≤13 s) and longest (≥100 s) periods the effective smoothing strength was greater because of the sparser path coverage at these periods.

Fig. 4 shows the phase-velocity maps including the 2Ψ anisotropy. We have allowed for 4Ψ heterogeneity in inversions as well but found that the resulting 4Ψ-anisotropy patterns are not robust. We have verified, however, that the isotropic and 2Ψ structure that we retrieve is robust with respect to the amount of the 4Ψ signal allowed in the

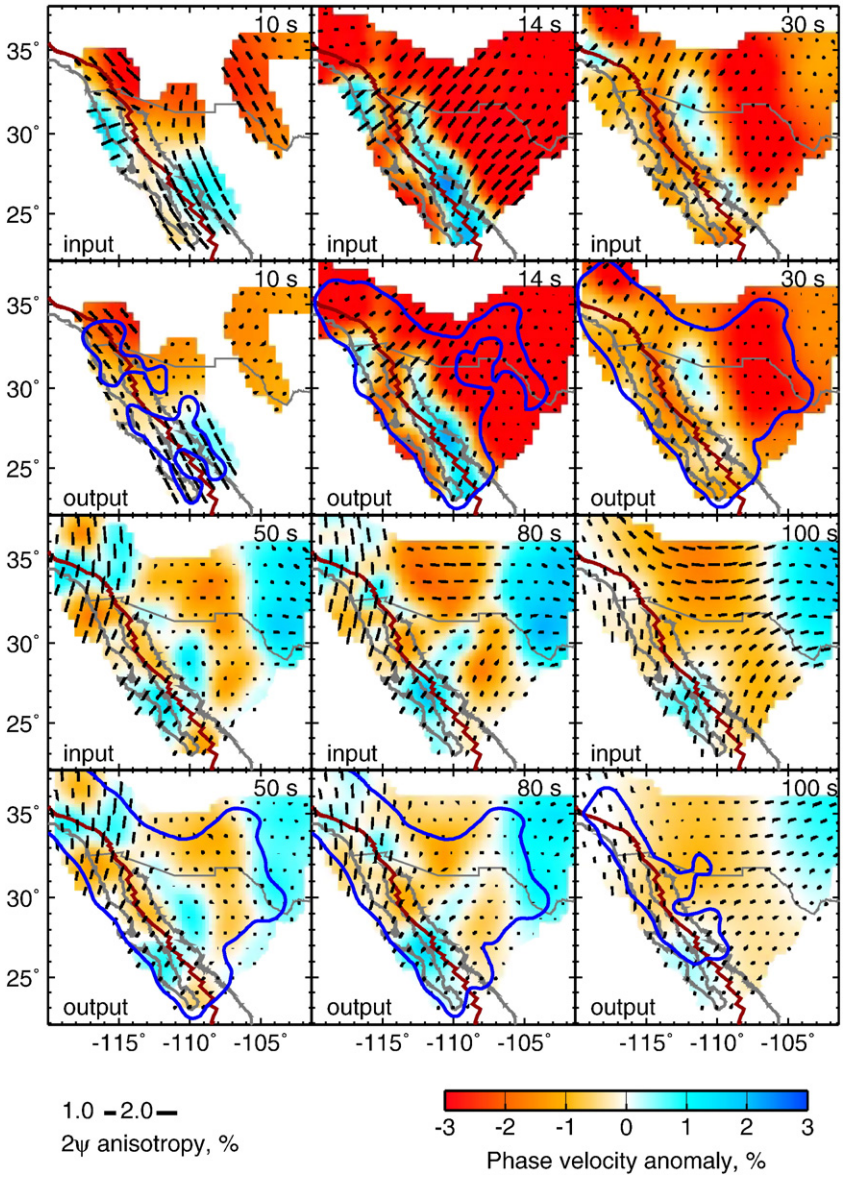

Fig. 5. A resolution test. The resolution test was performed by inverting a synthetic data set created from a model with isotropic coefficients taken from the real inversion result and 2Ψ-anisotropic coefficients such that the anisotropy was with the same strength but with fast-propagation directions perpendicular to those of the inversion result. The blue contours delineate the regions of high resolution (see text) in the original phase velocity maps.

models by the regularization. The isotropic and 2Ψ structure changed very little with 4Ψ signal strength changing in the range from zero to as high as that of the 2Ψ signal. Having calculated resolution matrices, we defined the well-resolved parts of the region as those containing the grid points with its diagonal elements of the isotropic term of the resolution matrix above 0.1 (Zhang et al., 2007). We also performed several resolution tests to verify the robustness of our results. Fig. 5 presents one of such tests. The input interstation phase velocities were calculated using models with isotropic terms taken from the actual phase velocity results as in Fig. 5, and 2Ψ anisotropic terms were such that the anisotropy was of the same strength but with a fast-propagation directions perpendicular to those in the actual phase velocity maps. Fig. 5 shows that the isotropic structure is reliably recovered and is not affected by the 2Ψ structure. The 2Ψ anisotropic terms are also recovered, except in peripheral regions with poor ray coverage. The accurate recovery of the anisotropic structure in this rigorous test confirms that our azimuthal path coverage is sufficient to constrain phase-velocity heterogeneity in the region of the study. The resolution length for the isotropic structure is estimated at 150–200 km in the best resolved area around the gulf. In order to evaluate the uncertainties of the phase velocity maps, we have calculated the posterior model covariance matrices. The square roots of the diagonal elements of the posterior model covariance matrices can be interpreted as the standard deviations of the estimated model parameters, i.e. the phase velocity perturbations at the grid points (Tarantola, 1987). The uncertainties of the isotropic phase velocity perturbations range from 0.7% (middle periods) to 1.3%(short and long periods). The differences are mainly due to the variations in path coverage and differences in smoothing.

The phase velocity maps of this study are very similar to the phase velocity maps of Zhang et al. (2007) in the region of overlap. The isotropic phase velocity structure of the two studies is nearly identical, although the current study covers a larger area. Slight changes in the anisotropic structure are observed along the peripheral regions of the first study; they are due to the enhanced path coverage in this study.

Having mapped anisotropic heterogeneity, we can isolate the isotropic phase-speed variations that are related to thermal and compositional structure of the mantle. We now invert the isotropic phase velocities for shear-speed structure. For this, the local phase velocity curve is estimated at each of the 182 points of the 100 km spaced geographical grid. These curves are then inverted for 1-D shear-velocity models using a non-linear gradient search method. The 1-D profiles are combined into a 3-D shear-velocity structure. The starting models for the inversions were obtained from the reference model AK135 (Kennett et al., 1995) for the mantle structure, combined with a local crustal structure. We used various sources to infer the local crustal shear velocity and the Moho depth: the Southern California velocity model SCEC-CVM-H (Süss and Shaw, 2003), receiver function studies (Zhu and Kanamori, 2000; Lewis et al., 2001; Persaud et al., 2007), seismic refraction studies (González-Fernández et al., 2005; Lizarralde et al., 2007), and the global crustal model CRUST2.0 (Bassin et al., 2000). Locations with various types of constraints on crustal structure are shown in Fig. 6, together with the resulting map of the crustal thickness that was used in the starting models.

We used 15 free parameters to expand shear speed variations down to 1000 km depth. Of the 15 parameters, one is a boxcar in shape and spans the crustal depth range; 11 are triangular basis functions parameterising mantle structure, with denser sampling at shallower mantle depths; 3 more parameters allow depth perturbations of the Moho, 410-km and 660-km discontinuities. Our phase velocity data have some sensitivity below 300 km, but as the period increases the uncertainty of the measurements increases and the depth resolution decreases. Therefore, we only show the upper 300 km of the model.

3. Results and interpretation

The results of the inversion are shown by the crustal thickness and the upper mantle shear-speed anomalies relative to the global reference model AK135 (Fig. 7). Seismic velocities in the upper mantle are much lower than global averages, especially at mantle depths down to 150–200 km. This has been seen previously in tomographic models that included the area (e.g. Lebedev and van der Hilst, 2008; Nettles and Dziewonski, 2008; van der Lee and Frederiksen, 2005; Godey et al., 2003). The low velocities point to the presence of fluids and/or melt (Goes and van der Lee, 2002). This can be due to the dehydration and/or partial melting from subducted lithosphere, decompression melting because of the opening of a slab window, or partial melting because of high temperatures. Recognizing the existence of very low shear velocities region-wide, we concentrate in the following on the lateral variations within the region.

A striking feature that we identify in this study is a relatively high velocity anomaly beneath the south–central part of the Gulf of California at depths between roughly 120 and 160 km (Fig. 7). We illustrate the difference in shear velocity beneath the northern and

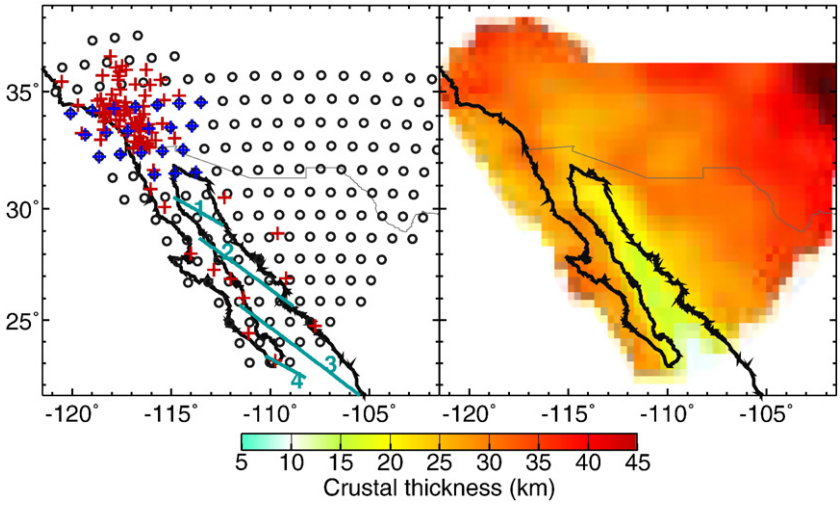

Fig. 6. Construction of the initial crustal model. In the frame on the left, the black circles indicate the grid used to parameterize the inversion; the blue lines indicate seismic reflection lines (González-Fernández et al., 2005; Lizarralde et al., 2007); the red crosses indicate the locations with receiver function data (Zhu and Kanamori, 2000; Lewis et al., 2001; Persaud et al., 2007); the blue crosses indicate the area covered by the SCEC-CVM-H model (Süss and Shaw, 2003). The frame on the right shows the crustal thickness in our initial crustal model based on this data. Where no other information is available, Crust2.0 (Bassin et al., 2000) is adopted.

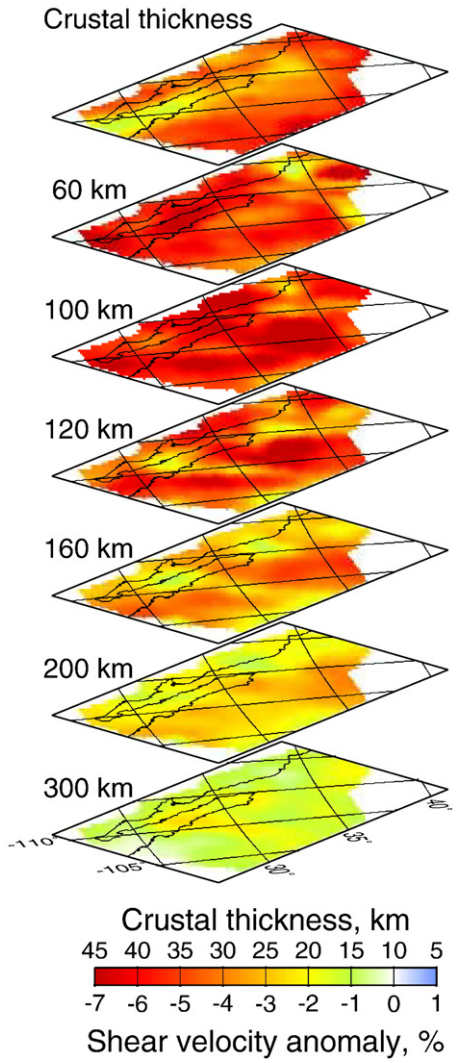

Fig. 7. Maps of the crustal thickness (upper panel), and the shear velocity anomalies relative to the global reference model AK135 (Kennett et al., 1995) at depths of 60, 100, 120, 160, 200, and 300 km.

southern gulf more closely by comparing two selected grid points in these areas. Fig. 8 shows their locations, phase velocity curves and 1-D velocity structures. Note that the phase velocity curves do not overlap within the error bars in the 60–90 s period range. The shear velocity structure for the northern grid point shows a thin lid overlying a pronounced low velocity layer. Except for the thin lid this velocity structure is very similar to the average shear velocity structure beneath southern California obtained by Yang and Forsyth (2006). The shear velocity structure for the southern grid point does not show a clear lid and has significantly higher velocities in the 100–200 km depth range. The absence of the lid may be related to the fact that this grid point is located right above the active rift. More important however are the relatively high velocities in the 100–200 km depth range (albeit smaller than AK135). These velocities are not only several percent higher than those of the northern grid point, but also compared to the shear velocities beneath the East Pacific Rise (Webb and Forsyth, 1998).

Errors in the crustal thickness may affect the inferred velocity structure. However, the Moho depth in the gulf is well constrained from seismic refraction experiments (see Fig. 6). Since we further allow the crustal thickness to vary in the inversion, we believe that the estimated velocity structure is not significantly affected by Moho depth uncertainties, and certainly not at depths larger than 100 km.

We interpret the high velocity anomaly in the 120–160 km depth range beneath the south–central gulf as a remnant slab fragment, for two reasons: (1) it is a relatively high shear-velocity anomaly in an area of former microplate subduction, and (2) volcanism in the region, above the anomaly, shows a clear slab signature (Pallares et al., 2007; Bellon et al., 2006; Conly et al., 2005). The crucial point for the tectonic interpretation of this feature is the origin of the slab. Although its current location is just east of the unsubducted portion of the Magdalena microplate we attribute this anomaly to the Guadalupe microplate. The part of the latter that last subducted comprised older and, therefore, colder oceanic lithosphere and can be expected to be more visible in the shear-speed image. The North–South extent of the anomaly matches the width of the Guadalupe plate between the Guadalupe and Shirley fracture zones (Fig. 1). Moreover, according to plate-tectonic reconstructions, at the time when the Guadalupe microplate ceased to subduct its location relative to Baja California was where we currently find the high velocity anomaly (Lonsdale, 1991; Stock and Lee, 1994).

Our conclusion that the anomaly is a remnant of the Guadalupe slab has important consequences. It implies that in the last 12 Ma this slab remnant has not moved noticeably relative to the overlying Baja California, whereas the unsubducted part of the Guadalupe microplate moved together with the Pacific plate roughly 300 km to the northwest (Spencer and Normark, 1989; Oskin and Stock, 2003) to its present location (Fig. 1). We propose that the Guadalupe slab broke off at depth beneath the current location of the Gulf of California, i.e. at the eastern margin of the relative high velocity anomaly. Because of the removal of the slab pull force, subduction stopped and spreading ceased. The

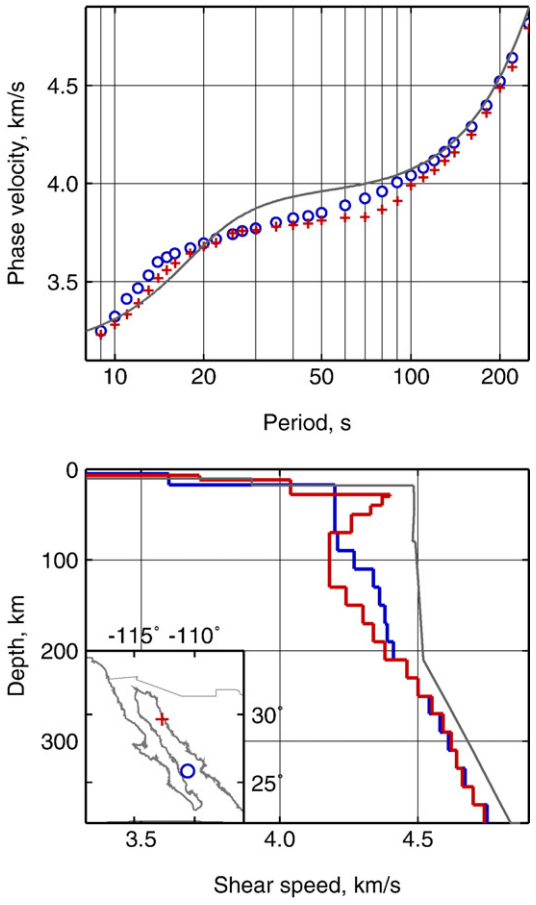

Fig. 8. Phase velocity curves (upper panel) and the inverted shear velocity structures (lower panel) at two grid points. The locations of the two grid points are depicted in the lower left corner of the lower panel. The gray lines are for global reference model AK135 (Kennett et al., 1995).

western part of the Guadalupe oceanic plate was effectively captured by the Pacific Plate, and the Guadalupe–North American relative movement became the same as the Pacific–North American movement, of a predominantly strike-slip character. This new Pacific–North American transcurrent motion was taken up by San Benito and Tosco–Abreojos transform faults that developed next to the (inactive) trench. These faults must have cut through the subducted remnant of Guadalupe lithosphere that was now stalled in the uppermost mantle beneath Baja California, leaving the remnant completely detached from its origin.

Our interpretation of the origin of this shear-velocity anomaly and the tectonic reconstruction are further supported by the analysis of magmatism in Baja California and the gulf. Much of the volcanism in Baja California since 12 Ma occurred in fields at latitudes between 26° and 27.5°N. Some of the lavas have been associated with partial melting of oceanic crust (adakites), others with a mantle metasomatized by slab-derived aqueous fluids (andesites), and others yet were identified as tholeiitic basalts similar to mid-ocean ridge basalts (MORBs) or ocean island basalts (OIBs) (e.g., Sawlan, 1991; Conly et al., 2005; Pallares et al., 2007). The adakites are best accounted for by melting at the edges of the slab remnant, whereas the andesites originate from the supra-slab mantle metasomatized by slab melts. The tholeiites, on the other hand, are produced in regions without a slab remnant. The limited lateral extend of the slab remnant explains the close proximity of these types of volcanism in central Baja California.

We note further, that our results show very low shear velocities in the central region of the gulf at depths of approximately 60 km. This is the location above the high-velocity anomaly, so that these low velocities are most likely associated to supra-slab mantle metasomatized by slab-derived aqueous fluids and melts. Based on volcanic evidence and tectonic reconstructions, various geometries of subducted slab fragments and asthenospheric slab windows have been proposed in previous studies (Pallares et al., 2007; Fletcher et al., 2007; Conly et al., 2005; Ferrari, 2004; Benoit et al., 2002). None of the scenarios, however, proposed a slab remnant that is localized in the central region of the Gulf as is found in our tomographic results.

Through its effect on magmatism, the remnant slab may also control the character of the rifting—reflected, in particular, in the thickness of the crust. The crust in our model is thinner in the southern part of the gulf than in the northern part, which is in agreement with previous studies (Lizarralde et al., 2007; González-Fernández et al., 2005). More importantly, we find a conspicuous geographical correspondence between the northernmost extent of the thin-crusted portion of the gulf and the northern boundary of the slab remnant (relatively high-velocity feature) in the central gulf. The variations in crustal thickness appear to correspond to the variations in volcanism, and the variations of both types may be related to the change from the presence of the slab remnant in the south–central part to its absence in the northern part of the gulf. The Guaymas basin (along refraction line 2 in Fig. 6), located above the relatively high velocity feature, is a narrow rift with very high magma production since the opening of the gulf (Lizarralde et al., 2007). This is anomalous because the primary style of rifting in the rest of the gulf is close to that of a wide rift with low melt generation (Lizarralde et al., 2007; González-Fernández et al., 2005). The more southerly Alarcon basin (along refraction line 3 in Fig. 6), for instance, experienced ca. 350 km of continental extension before seafloor spreading started 2–3 Myr ago, probably fed by the magmatic source from the East Pacific Rise (Lizarralde et al., 2007). The voluminous magmatism in the Guaymas basin since its opening (Batiza, 1978; Lizarralde et al., 2007) can be explained by the slab break-off and the presence of the stalled slab fragment which enriched the mantle. Furthermore, magmatic weakening of the lithosphere by the stalled slab fragment may have contributed and resulted in the sea-floor spreading in the central Gulf of California, occurring in contrast to the diffuse extension just to the North (González-Fernández et al., 2005; Lizarralde et al., 2007).

Our results also show other anomalies such as a thin crust in the Salton Sea area and relatively fast shear-velocity anomalies beneath the Transverse Ranges. These features have been found in previous surface wave studies that focused on southern California (Yang and Forsyth, 2006; Prindle and Tanimoto, 2006). The thin crust of the Salton Sea is associated with lithospheric extension; it defines the northern part of the Gulf Extensional Province. The fast anomalies beneath the Transverse Ranges have been related to lithospheric down-welling.

4. Conclusion

The Gulf of California exhibits different stages of the transition from continental rifting to seafloor spreading. Its northern part is characterized by diffuse continental extension, whereas the southern part contains oceanic spreading centers and transform faults. We determined the crustal and upper mantle shear-speed structure using Rayleigh wave dispersion measurements. Measured phase-velocity curves were inverted for phase velocity maps which were then inverted for shear-speed structure. The high resolution of our tomography has been enabled by the newly available data, largely from the stations of the NARS–Baja network deployed around the gulf.

The shear-speed model shows a relatively fast anomaly in the upper mantle with overall low shear velocities. The anomaly, which is well-resolved in the central part of the gulf at depths approximately between 120 and 160 km, is interpreted as a remnant of the subducted Guadalupe plate, a Farallon-derived microplate. The current location of the anomaly implies that the slab fragment has been stalled beneath Baja California since 12 Ma, and strongly influenced the evolution of the gulf. Its presence, in particular, can account for the variability in the magmatism in central Baja California.

We attribute the location of the transition from continental extension (North) to oceanic spreading (South) in the Gulf of California to the location of the slab remnant, present beneath the central–southern part and absent beneath the northern part. It is therefore concluded that the complex tectonics related to the cessation of Farallon subduction has governed the evolution of the gulf.

Acknowledgments

We thank the people who supported the NARS–Baja project: Jeannot Trampert, Arie van Wettum (Utrecht University), Robert Clayton (Caltech), Raul Castro and Arturo Perez-Vertti (CICESE). Funding for this project was provided by the Utrecht University, the Dutch National Science Foundation (Grant number NWO-GOA-750.396.01) and the U.S. National Science Foundation (Grant number EAR-0111650 of the MARGINS program). Maintenance of the CICESE broadband stations is partly funded by CONACYT Project 37038-T. The data used in this research were partly obtained from the IRIS Data Management Center. We would like to thank the following networks: the Caltech Regional Seismic Network(CI) from California Institute of Technology; the IRIS/IDA Network(II) from University of California, Scripps Institute of Oceanography; the IRIS/USGS Network(IU) from USGS Albuquerque Seismological Laboratory; the Leo Brady Network (LB) from Sandia National Laboratory; the USArray Transportable Array (TA) from Earthscope Project; the US National Seismic Network (US) from ANSS Backbone of the USGS/NEIC and USGS/ASL and Earthscope Project of IRIS. We thank Helle Pedersen and an anonymous reviewer for their careful reviews. Their suggestions have improved this manuscript.

References

Aguillón-Robles, A., Calmus, T., Benoit, M., Bellon, H., Maury, R., Cotten, J., Bourgois, J., Michaud, F., 2001. Late Miocene adakites and Nb-enriched basalts from Vizcaino Peninsula, Mexico: indicators of East Pacific Rise subduction below southern Baja California? Geology 29, 531–534.

Atwater, T., Stock, J.M., 1998. Pacific–North America plate tectonics of the Neogene Southwestern United States: an Update. Int. Geol. Rev. 40, 375–402.
Bassin, C., Laske, G., Masters, G., 2000. The Current Limits Of Resolution For Surface Wave Tomography In North America. EOS Trans. AGU F897.
Batiza, R., 1978. Geology, petrology, and geochemistry of Isla Tortuga, a recently formed tholeiitic island in the Gulf of California. Geol. Soc. Am. Bull. 89, 1309–1324.
Bellon, H., Aguillón-Robles, A., Calmus, T., Maury, R., Bourgois, J., Cotten, J., 2006. La Purisima volcanic field, Baja California Sur, Mexico: Mid-Miocene to Recent volcanism in relation with subduction and asthenospheric window opening. J. Volcanol. Geotherm. Res. 152, 253–272.
Benoit, M., Aguillón-Robles, A., Calmus, T., Maury, R., Bellon, H., Cotten, J., Bourgois, J., Michaud, F., 2002. Geochemical diversity of Late Miocene volcanism in southern Baja California, Mexico: implication of mantle and crustal sources during the opening of an asthenospheric window. J. Geol. 110, 627–648.
Calmus, T., Aguillón-Robles, A., Maury, R., Bellon, H., Benoit, M., Cotten, J., Bourgois, J., Michaud, F., 2003. Spatial and temporal evolution of basalts and magnesian andesites ("bajaites") from Baja California, Mexico: the role of slab melts. Lithos 66, 77–105.
Conly, A., Brenan, J., Bellon, H., Scott, S., 2005. Arc to rift transitional volcanism in the Santa Rosalía Region, Baja California Sur, Mexico. J. Volcanol. Geotherm. Res. 142, 303–341.
Dickinson, W., Snyder, W., 1979. Geometry of subducted slabs related to San Andreas transform. J. Geol. 87, 609–627.
Ferrari, L., 2004. Slab detachment control on mafic volcanic pulses and mantle heterogeneity in central Mexico. Geology 32, 77–80.
Fletcher, J.M., Grove, M., Kimbrough, D., Lovera, O., Gehrels, G.E., 2007. Ridge-trench interactions and the Neogene tectonic evolution of the Magdalena shelf and southern Gulf of California: insights from detrital zircon U-Pb ages from the Magdalena fan and adjacent areas. GSA Bulletin 119, 1313–1336. doi:10.1130/B26067.1.
Gastil, G., Krummenacher, D., Minch, J., 1979. The record of Cenozoic volcanism around the Gulf of California. GSA Bulletin 90, 839–857.
Godey, S., Snieder, R.K., Villaseñor, A., Benz, H.M., 2003. Surface wave tomography of North America and the Caribbean using global and regional broad-band networks: phase velocity maps and limitations of ray theory. Geophys. J. Int. 152, 620–632.
Goes, S., van der Lee, S., 2002. Thermal structure of the North American uppermost mantle inferred from seismic tomography. J. Geophys. Res. 107 (B32050). doi:10:1029/2000JB000049.
González-Fernández, A., Dañobeitia, J.J., Delgado-Argote, L.A., Michaud, F., Córdoba, D., Bartolomé, R., 2005. Mode of extension and rifting history of upper Tiburón and upper Delfín basins, northern Gulf of California. J. Geophys. Res. 110 (B01313). doi:10.1029/2003JB002941.
Gripp, A.E., Gordon, R.G., 2002. Young tracks of hotspots and current plate velocities. Geophys. J. Int. 150, 321–361.
Hausback, B.P., 1984. Cenozoic volcanism and tectonic evolution of Baja California Sur, Mexico. In: Frizell, V.A. (Ed.), Geology of the Baja California Peninsula: Pacific Section. Soc. Eco. Pal. and Min., vol. 39. Los Angeles, California, pp. 219–236.
Henry, C.D., Aranda-Gomez, J.J., 2000. Plate interactions control middle–late Miocene proto-Gulf and basin and range extension in the southern basin and range. Tectonophysics 318, 1–26.
Karig, D.E., Jensky, W., 1972. The proto-Gulf of California. Earth Planet. Sci. Lett. 17, 169–174.
Kennett, B.L.N., Engdahl, E.R., Buland, R., 1995. Constraints on seismic velocities in the earth from travel times. Geophys. J. Int. 122, 108–124.
Lebedev, S., van der Hilst, R.D., 2008. Global upper-mantle tomography with the automated multimode inversion of surface and S-wave forms. Geophys. J. Int. 173, 505–518. doi:10.1111/j.1365–246X.2008.03721.x.
Lebedev, S., Nolet, G., Meier, T., van der Hilst, R.D., 2005. Automated multimode inversion of surface and S waveforms. Geophys. J. Int. 162, 951–964. doi:10.1111/j.1365–246X.2005.02708.x.
Lewis, J.L., Day, S.M., Magistrale, H., Castro, R.R., Astiz, L., Rebollar, C., Eakins, J., Vernon, F.L., Brune, J.N., 2001. Crustal thickness of the Peninsular Ranges and Gulf Extensional Province in the Californias. J. Geophys. Res. 106 (B7), 13599–13611.
Lizarralde, D., Axen, G.J., Brown, H.E., Fletcher, J.M., González-Fernández, A., Harding, A. J., Holbrook, W.S., Kent, G.M., Paramo, P., Suther, F., Umhoefer, P.J., 2007. Variation in styles of rifting in the Gulf of California. Nature 448, 466–469. doi:10.1038/nature06035.
Lonsdale, P., 1989. Geology and tectonic history of the Gulf of California. In: Hussong, D., Winterer, E.L., Decker, R.W. (Eds.), The Eastern Pacific Ocean and Hawaii. The Geology of North America, vol. N. Geological Society of America, Boulder, Colorado, pp. 499–521.
Lonsdale, P., 1991. Structural patterns of the Pacific floor offshore of peninsular California. In: Dauphin, J.P., Simoneit, B.R.T. (Eds.), The Gulf and Peninsular Province of the Californias, vol. 47. AAPG Memoir, pp. 87–125.
Mammerickx, J., Klitgord, K.D., 1982. Northern East Pacific rise: evolution from 25 m.y. B. P. to the present. J. Geophys. Res. 87, 6751–6759.
Meier, T., Dietrich, K., Stockhert, B., Harjes, H.P., 2004. One-dimensional models of shear wave velocity for the eastern Mediterranean obtained from the inversion of Rayleigh wave phase velocities and tectonic implications. Geophys. J. Int. 156, 45–58.
Michaud, F., Royer, J.-Y., Bourgois, J., Dyment, J., Calmus, T., Bandy, W., Sosson, M., Mortera-Gutiérrez, C., Sichler, B., Rebolledo-Viera, M., Pontoise, B., 2006. Oceanic–ridge subduction vs. slab break-off: plate tectonic evolution along the Baja California Sur continental margin since 15 Ma. Geology 34, 13–16.
Nagy, E.A., Stock, J.M., 2000. Structural controls on the continent–ocean transition in the northern Gulf of California. J. Geophys. Res. 105 (B7), 16,251–16,269.
Nettles, M., Dziewonski, A.M., 2008. Radially anisotropic shear velocity structure of the upper mantle globally and beneath North America. J. Geophys. Res. 113 (B02303). doi:10.1029/2006JB004819.
Oskin, M., Stock, J., 2003. Miocene to Recent Pacific–North America plate motion and opening of the Upper Delfín Basin, northern Gulf of California, Mexico. Geol. Soc. Amer. Bull. 115, 1173–1190.
Paige, C., Saunders, M., 1982. LSQR: an algorithm for sparse linear equations and sparse least squares. ACM. Trans. Math. Softw. 8, 43–71.
Pallares, C., Maury, R.C., Bellon, H., Royer, J.Y., Calmus, T., Aguillón-Robles, A., Cotten, J., Benoit, M., Michaud, F., Bourgois, J., 2007. Slab-tearing following ridge-trench collision: evidence from Miocene volcanism in Baja California, México. J. Volcanol. Geotherm. Res. 161, 95–117. doi:10.1016/j.jvolgeores.2006.11.002.
Pedersen, H.A., 2006. Impacts of non-plane waves on two-station measurements of phase velocities. Geophys. J. Int. 165, 279–287. doi:10.1111/j.1365–246X.2006.02893.x.
Persaud, P., Stock, J.M., Steckler, M.S., Martin-Barajas, A., Diebold, J.B., González-Fernández, A., Mountain, G.S., 2003. Active deformation and shallow structure of the Wagner, Consag, and Delfín Basins, northern Gulf of California, Mexico. J. Geophys. Res. 108 (B7), 2355. doi:10.1029/2002JB001937.
Persaud, P., Pérez-Campos, X., Clayton, R.W., 2007. Crustal thickness variations in the margins of the Gulf of California from receiver functions. Geophys. J. Int. 170, 687-669. doi:10.1111/j.1365–246X.2007.03412.x.
Plattner, C., Malservisi, R., Dixon, T., Sella, G., Lafemina, P., Fletcher, J., Suarez-Vidal, F., 2007. New constraints on relative motion between the Pacific plate and Baja California microplate (Mexico) from GPS measurements. Geophys. J. Int. 1373–1380. doi:10.1111/j.1365–246X.2007.03494.x.
Prindle, K., Tanimoto, T., 2006. Teleseismic surface wave study for S–wave velocity structure under an array: Southern California. Geophys. J. Int. 166, 601–621. doi:10.1111/j.1365–246X.2006.02947.x.
Sawlan, M.G., 1991. Magmatic evolution of the Gulf of California rift. In: Dauphin, J.P., Simoneit, B.R.T. (Eds.), The Gulf and Peninsular Province of the Californias, vol. Memoir 47. The American Association of Petroleum Geologists, Tulsa, OK, pp. 301–370.
Sawlan, M.G., Smith, J.G., 1984. Petrologic characteristics, age and tectonic setting of Neogene volcanic rocks in northern Baja California Sur, Mexico. In: Frizell, V.A. (Ed.), Geology of the Baja California Peninsula: Pacific Section. Soc. Eco. Pal. and Min., vol. 39. Los Angeles, California, pp. 237–251.
Süss, M.P., Shaw, J.H., 2003. P wave seismic velocity structure derived from sonic logs and industry reflection data in the Los Angeles basin, California. J. Geophys. Res. 108 (B32170). doi:10.1029/2001JB001628.
Severinghaus, J., Atwater, T.M., 1990. Cenozoic geometry and thermal state of the subducting slabs beneath North America. In: Wernicke, B.P. (Ed.), Basin and Range Extensional Tectonics Near the Latitude of Las Vegas, Nevada. Geol. Soc. Amer. Memoir, vol. 176. AGU, pp. 1–22.
Smith, M.L., Dahlen, F.A., 1973. The azimuthal dependence of Love and Rayleigh wave propagation in a slightly anisotropic medium. J. Geophys. Res. 78, 3321–3333.
Spencer, J., Normark, W., 1989. Neogene plate–tectonic evolution of the Baja California Sur continental margin and the southern Gulf of California, Mexico. In: Winterer, E., Hussong, D., Decker, R. (Eds.), The Geology of North America. The Eastern Pacific Ocean and Hawaii, vol. N. Geological Society of America, Boulder, Colorado, pp. 489–497.
Stock, J.M., Hodges, K.V., 1989. Pre-Pliocene extension around the Gulf of California and the transfer of Baja California to the Pacific Plate. Tectonics 8 (1), 99–115.
Stock, J.M., Lee, J., 1994. Do microplates in subduction zones leave a geological record? Tectonics 13 (6), 1472–1487.
Tarantola, A., 1987. Inverse Problem Theory: Methods for Data Fitting and Model Parameter Estimation. Elsevier, Amsterdam.
Trampert, J., A. van Wettum, J.R., Clayton, R., Castro, R., Rebollar, C., Perez-Vertti, A., 2003. New array monitors seismic activity near the Gulf of California in Mexico. Eos Trans. AGU 84 (4), 29–32.
van der Lee, S., Frederiksen, A., 2005. Surface wave tomography applied to the North American upper mantle. In: Nolet, G., Levander, A. (Eds.), Seismic Data Analysis and Imaging With Global and Local Arrays. Geophys. Monogr. Ser., vol. 157. AGU, Washington, D.C., pp. 67–80.
Webb, S.C., Forsyth, D.W., 1998. Structure of the upper mantle under the EPR from waveform inversion of regional events. Science 280, 1227–1229. doi:10.1126/science.280.5367.1227.
Yang, Y., Forsyth, D.W., 2006. Rayleigh wave phase velocities, small-scale convection, and azimuthal anisotropy beneath southern California. J. Geophys. Res. 111 (B07306). doi:10.1029/2005JB004180.
Zhang, X., Paulssen, H., Lebedev, S., Meier, T., 2007. Surface wave tomography of the Gulf of California. Geophys. Res. Lett. 34 (L15305). doi:10.1029/2007GL030631.
Zhu, L., Kanamori, H., 2000. Moho depth variation in southern California from teleseismic receiver functions. J. Geophys. Res. 105, 2969–2980.